

## Detection of an Annual Westward Propagating Signal in the Meridional Wind Component along 8°N in the Pacific

SHOSHIRO MINOBE

*Division of Earth and Planetary Sciences, Graduate School of Science, Hokkaido University, Sapporo, Japan*

(Manuscript received 18 November 1994, in final form 6 February 1996)

### ABSTRACT

A westward propagating signal with the annual period is detected in anomalies of the zonally averaged meridional wind component along 8°N across the Pacific Ocean. The propagating signal in the "eddy" (defined as the departure from the zonally averaged) meridional wind has approximately the same propagation speed as the well-known propagating signal in the zonal wind component along the equator, and the former has larger amplitude than the latter. The eddy SST gradient between the equator and 10°N exhibits a similar westward propagation and is in phase with the eddy meridional wind; the northward eddy wind is accompanied by the warmer eddy SST to the north. The propagating features in both the eddy meridional wind and the SST gradient are quite regular from year to year, except for El Niño years. In the El Niño periods, the regular features are disturbed in the western Pacific, but the in-phase relationship between these two parameters still holds. These relationships indicate that the boundary-layer mechanism is most likely to be of primary importance in the response of the eddy meridional wind to the SST variations.

### 1. Introduction

Atmospheric and oceanic seasonal variations in the tropical Pacific have been studied by many authors. An interesting phenomenon in those variations is annual westward propagating signals along the equator in both the atmosphere and ocean. Meyers (1979) reported that the annual harmonic of zonal wind stress propagates toward the west across the Pacific. Spectrum analysis by Lukas and Firing (1985) showed that the propagation is the dominant feature in the equatorial annual zonal wind stress. It is also well known that the annual period component of sea surface temperature (SST) anomaly propagates westward (Bjerknes 1961) and is closely related to the westward-propagating signal in the zonal wind stress. Horel (1982) first pointed out the possibility that the propagating signals in both fields might result from the interaction between the atmosphere and ocean. Recently, these propagating signals have attracted attention as evidence of the air–sea interaction on the seasonal timescale (e.g., Philander 1990; Philander and Chao 1991) and have been the subjects of observational studies (Murakami and Wang 1993; Wang 1994b) and theoretical and numerical studies (Meehl 1990; Xie 1994a; Chang and Philander 1994).

In contrast to the westward propagating signal in the zonal wind stress along the equator, the annual cycle of the extraequatorial zonal wind stress is dominated by the meridional migration of the trade wind belt (Wyrtki and Meyers 1976). The annual phase of the zonal wind speed is approximately uniform in each hemisphere poleward of 5° and is characterized by the maximum of eastward wind in each hemispheric summer (Fig. 1). The meridional wind has roughly uniform phase over the tropical Pacific, with the wind direction from the winter hemisphere to the summer hemisphere. Although the annual cycle of the wind fields are not dominated by these zonally uniform components in the southeastern tropical Pacific, the annual amplitudes of the zonal and meridional winds are small in this region. The zonally uniform components are therefore dominant in the meridional and extraequatorial zonal winds, and longitudinally uniform zonal and meridional winds are antisymmetric and symmetric about the equator, respectively. These features in the wind speed field are common in the wind stress field. The annual cycle of the zonally uniform components is due to the responses of an air–sea coupled mode forced by the differential solar insolation between the Northern and Southern Hemispheres, and the westward propagating feature in the zonal wind and SST near the equator is attributed to another air–sea coupled mode (e.g., Wang 1994b; Chang and Philander 1994).

The existence of a component of the wind with longitudinally uniform phase, however, does not preclude the existence of a significant propagating signals but indicates that the propagating signals in longitudinally

---

*Corresponding author address:* Dr. Shoshiro Minobe, Division of Earth and Planetary Sciences, Graduate School of Science, Hokkaido University, N10, W8 Sapporo 060, Japan.

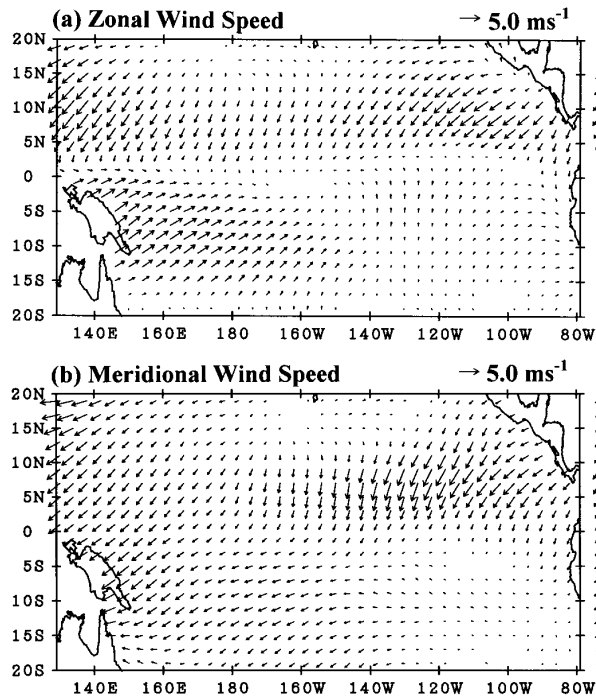


FIG. 1. Annual harmonic components of the (a) zonal and (b) meridional wind speeds. The vectors in the right margin indicate the longitudinally averaged annual harmonics of the respective wind fields. The amplitude of the annual cycle is indicated by the length of the arrow according to the scale in the figure. No arrow is plotted when the amplitude is less than  $1/20$  of the full scale ( $0.25 \text{ m s}^{-1}$ ). The phase is indicated by the direction of the arrow. An arrow pointing to the right indicates the eastward maximum for the zonal wind or northward maximum for the meridional wind on 1 January, to the top of the page on 1 April, etc.

dependent components must have smaller amplitude than the respective zonally uniform components. The equatorial westward propagating zonal wind anomaly, indicated as an anticlockwise rotation of the arrows toward the west in Fig. 1, has generally smaller amplitude than the zonally uniform wind components. In particular, both the longitudinally uniform zonal and meridional winds have the respective amplitude maxima of about  $3 \text{ m s}^{-1}$  around  $8^\circ\text{N}$ , whereas the rms amplitude of the zonal wind speed is about  $1 \text{ m s}^{-1}$  along the equator. Therefore, the amplitude of the extratropical propagating signal can be as large as the amplitude of the propagating signal along the equator. In order to understand the nature of air–sea coupled system, it is important to know the entire structure of the propagating components that might be obscured by more energetic zonally uniform components in the equatorial and extratropical Tropics.

Only a few studies have examined the propagating signals in the seasonal variations of the SST and wind fields by removing zonally uniform components. Horel (1982) found that the annual harmonic of the SST departure from the zonal mean propagates westward, not

only along the equator, but in the region between the equator and about  $15^\circ\text{S}$  in the Pacific. For the zonal wind speed, Mitchum and Lukas (1990) examined the latitudinal energy distribution of the annual harmonic of global wavenumber  $-3$ , which corresponds to the phase speed of the westward propagating signal along the equator. They reported that the energy peak is not at the equator but at  $7^\circ\text{N}$ , suggesting that the core of the propagating signal in the zonal wind stress is located away from the equator. However, they also showed that the zonal wind stress reconstructed from wavenumber components from  $-2$  to  $-4$  has larger amplitude over the Indian monsoon region and smaller amplitude over the central and eastern Pacific Ocean along  $7^\circ\text{N}$ . On the other hand, the equatorial propagating signal in zonal wind is prominent across the Pacific basin (Meyers 1979; Lukas and Firing 1985). Hence, the interaction between the equatorial and extratropical propagating signals is still unclear. The purpose of the present study is, therefore, to examine the presence of westward propagating signals in the zonally dependent seasonal variations of the wind and SST fields and to understand the relationships between the propagating signals.

The organization of the paper is as follows. In section 2, the data and method of analysis are described. The propagating signals detected in the zonally dependent components are described in section 3 for the wind and SST fields. These propagating signals are examined in terms of the relationships to the propagating signals studied in the previous papers in section 4. Summary and discussion are given in section 5.

## 2. Data and processing

The parameters investigated in this study are monthly means of zonal and meridional surface wind speeds and SST. The SST data were produced at the National Meteorological Center on monthly  $2^\circ \times 2^\circ$  grid from 1970 to 1984 (Reynolds 1983). The surface wind speeds are derived from wind pseudostress analyses produced at The Florida State University (FSU). The FSU wind fields are based on ship measurements binned into  $2^\circ \times 10^\circ$  latitude–longitude regions and then interpolated to a  $2^\circ \times 2^\circ$  grid (Goldenberg and O'Brien 1981). Although the FSU data are available from 1966 to 1989, we use the wind data during the same period as the SST data. Surface pseudostress was converted to surface wind speed, introducing a small error that should not significantly affect the results.

Two averages are removed from any variable,  $s$ . First, we ignore the longitudinally independent variation by removing the zonal mean over the tropical Pacific from  $130^\circ\text{E}$  and  $80^\circ\text{W}$ ,  $\hat{s}$ , at each latitude and month. Thus, departure from the zonal mean is given by

$$s^*(x, y, t) = s(x, y, t) - \hat{s}(y, t), \quad (1)$$

**Eddy Meridional Wind Speed (8°N)**

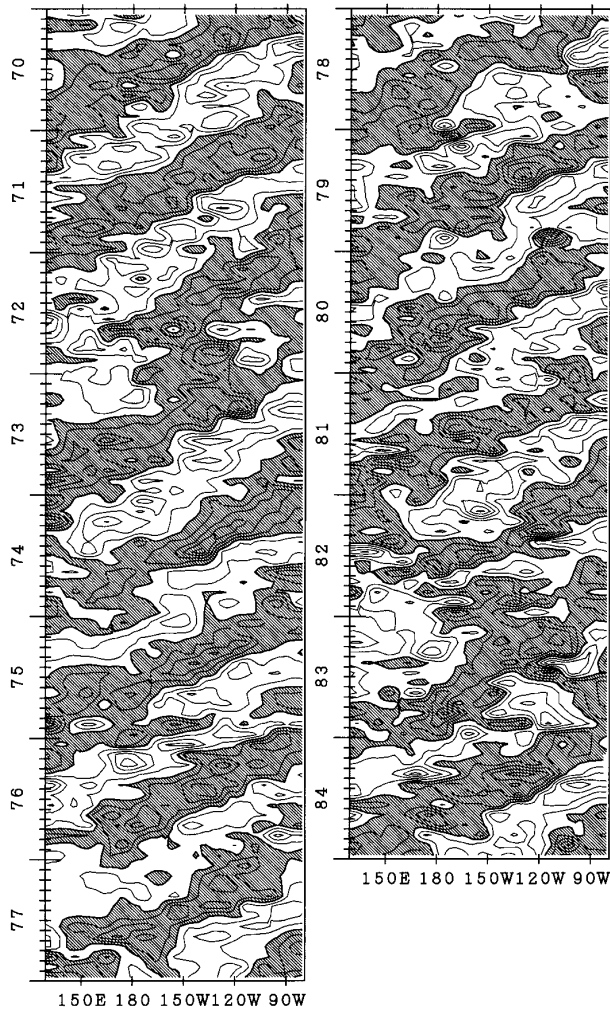


FIG. 2. Eddy surface meridional wind speed along 8°N from 1970 to 1984. Contour interval is 1 m s<sup>-1</sup>. Negative values are shaded.

where  $x$  and  $y$  are the longitude and latitude respectively,  $t$  is the time, the asterisk indicates the departure from the longitudinal mean, which is from now on referred to as eddy field, following Lindzen and Nigam (1987). Furthermore, in order to emphasize perturbations from the mean states, climatological annual means, that is, temporal averages over the record period, are removed from the eddy field. Therefore, the eddy monthly anomaly field,  $s'^*$ , is given by

$$s'^*(x, y, t) = s^*(x, y, t) - \bar{s}^*(x, y) \\ = s(x, y, t) - \hat{s}(y, t) - \bar{s}(x, y) + \hat{s}(y), \quad (2)$$

where prime indicates the anomaly from the climatological annual mean, which is denoted by an overbar. For simplicity, we henceforth use the term “eddy field” to describe the eddy monthly anomaly field un-

less otherwise stated. All the variables are smoothed with a 10° running mean in longitude, since we are interested in basin-scale phenomena.

**3. Propagating signals in wind and SST**

We examine whether the eddy zonal and meridional wind components exhibit propagating features at the annual period between 30°N and 30°S. The most prominent propagating signal is detected in the eddy meridional wind ( $v'^*$ ) along 8°N, as shown in Fig. 2. The propagating feature is remarkably regular from year to year. However, the propagating signals are disturbed in the western Pacific in association with El Niño events. This is shown by the positive anomalies to the west of the date line in autumn and winter associated with the 1972/73, 1976/77, and 1982/83 El Niños, whereas negative anomalies are dominant in this region in the autumn and winter of non El Niño years. Figure 3 shows the climatology of the eddy meridional wind along 8°N. The climatology is calculated from the data in individual years by averaging the data for each calendar month. A positive (negative) anomaly starts from the eastern side of the Pacific in May (December)

**Eddy  $v$  (8°N)**

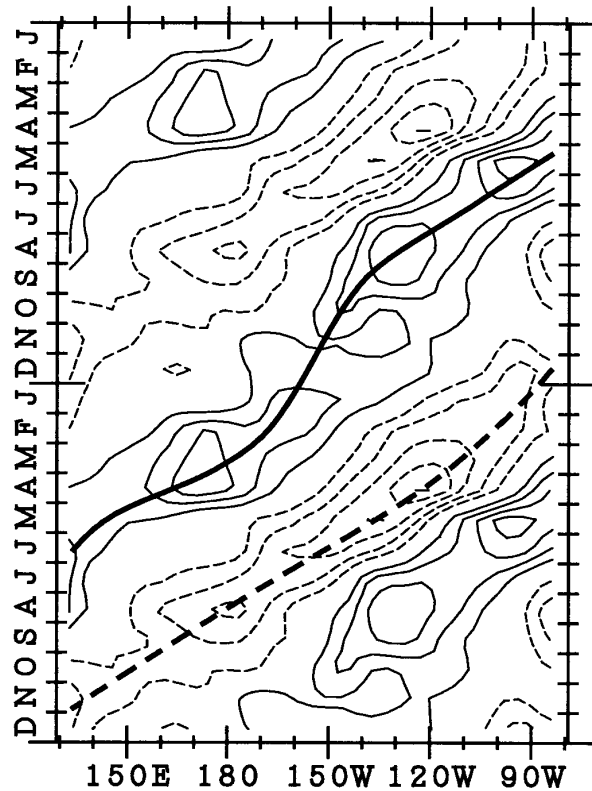


FIG. 3. Climatological monthly means of the eddy surface meridional wind speed for two years along 8°N. Contour interval is 0.5 m s<sup>-1</sup>, and zero contours are not shown.

and reaches the western side in June (November) of the next year, taking approximately one year to cross the basin. The meridional extent of the signal is roughly from  $4^\circ$  to  $12^\circ\text{N}$ . The existence of this propagating feature is also confirmed by the climatological wind velocity field produced by Sadler et al. (1987). The rms annual amplitude of the eddy meridional wind is  $1.22\text{ m s}^{-1}$ , which is larger than the rms amplitude of the equatorial eddy zonal wind of  $0.82\text{ m s}^{-1}$  ( $0.93\text{ m s}^{-1}$  when the zonal mean is not eliminated). In other words, the extraequatorial zonally propagating signal in the eddy meridional wind has larger amplitude than the well-known propagating annual component of the zonal wind speed along the equator. In the eddy zonal wind field, although the longitudinally uniform seasonal variation has been eliminated, a propagating signal is still found only along the equator. In the Southern Hemisphere, a basin-scale propagating signal is observed in neither the eddy zonal nor in meridional wind components.

In order to show the relation between the eddy and zonally uniform components of the meridional wind along  $8^\circ\text{N}$ , we plot the annual complex amplitude of the meridional wind speed on a complex plane (Fig. 4). The complex amplitude,  $\tilde{v}$ , is defined so that the variation due to the annual harmonic is represented as the real part of  $\tilde{v}e^{-i\omega t}$ , where  $\omega$  is the annual frequency and the tilde denotes the complex amplitude. The trajectory of the complex amplitude makes a distinctive anticlockwise circular pattern with approximately one revolution, as one moves westward across the Pacific. The anticlockwise rotation of the trajectory around the zonally uniform amplitude,  $\hat{v}$ , indicates westward phase increase, that is, the westward phase propagation, in the eddy field,  $\tilde{v}^*$ . The total phase with respect to the origin, however, does not continuously increase toward the west across the Pacific since the origin is not included inside the trajectory. The amplitude of the eddy component is about 40% of the amplitude of the zonally uniform component, indicating that the propagating signal is obscured by the 2.5 times larger longitudinally independent component. The wavelength of the eddy component is about  $130^\circ$  in longitude. This wavelength corresponds to a propagation speed of  $0.45\text{ m s}^{-1}$ , which is approximately the same as the propagation speed for the equatorial zonal wind evaluated by Meyers (1979) and Lukas and Firing (1985).

The seasonal atmospheric variations over the tropical Pacific are expected to be strongly influenced by the SST variations. An important mechanism in the propagating equatorial zonal wind is considered to be boundary-layer response (e.g., Horel 1982; Murakami and Wang 1993; Xie 1994a). In this case, the boundary-layer air temperature and density are modified by SST through surface boundary-layer fluxes, so that the pressure perturbation induced by the density perturbation is negatively correlated with the SST perturbation. Therefore, the pressure gradient forces the winds to

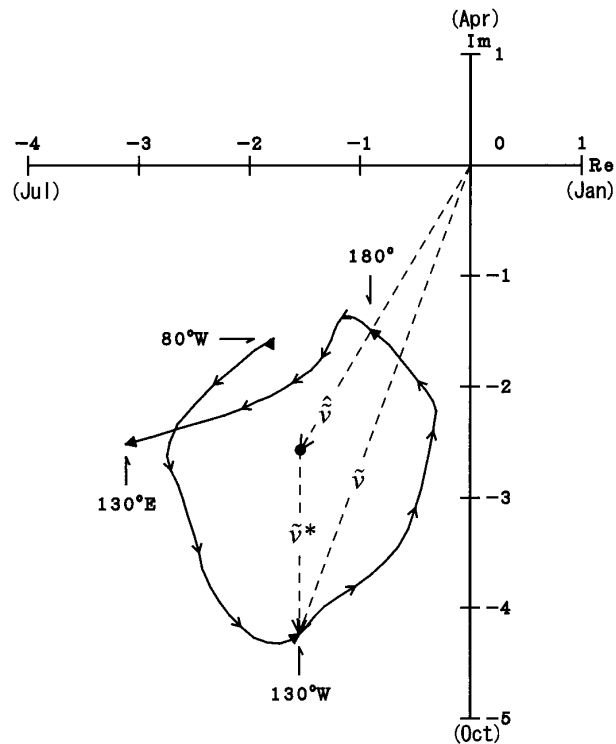


FIG. 4. Annual complex amplitude of the surface meridional wind speed,  $\tilde{v}$ , at  $8^\circ\text{N}$  as a function of longitude. The arrows are drawn for every  $10^\circ$  in longitude toward the west. The dot mark indicates the complex amplitude of the zonally uniform component,  $\hat{v}$ , and the relative position of the trajectory of the total amplitude with respect to the dot mark is the complex amplitude of the eddy field,  $\tilde{v}^*$ . The relationship among the  $\tilde{v}$ ,  $\tilde{v}^*$ , and  $\hat{v}$  is exemplified for those at  $130^\circ\text{W}$ . The argument of the complex amplitude is the annual phase; phase zero refers to the maximum on 1 January, the phase of  $90^\circ$  refers to the maximum on 1 April, and so on. As one moves westward across the Pacific basin, the trajectory rotates anticlockwise around the dot mark, indicating westward phase increase and, hence, the westward propagation in the eddy field.

blow down gradient, namely, the winds are forced to blow from a colder SST region to a warmer SST region (Lindzen and Nigam 1987). Figure 5 shows that a propagating signal is also detected in the eddy SST gradient between  $10^\circ\text{N}$  and the equator. The signal is as regular as that in the eddy meridional wind component along  $8^\circ\text{N}$ . These two variables are generally in phase, as evidenced by comparing Fig. 3 and Fig. 6a for the climatologies. In other words, the eddy wind blows northward when the northern eddy SST is warmer than the equatorial eddy SST. This phase relation is consistent with an interpretation of the wind perturbation as the response of the boundary-layer processes. As well as the propagating signal in the eddy meridional wind speed, the propagating feature in the eddy SST gradient is disturbed by El Niño events in the western Pacific. In the mature stage of El Niños, the SST in the eastern Pacific is warmer than normal, yielding positive and negative eddy SST in the eastern

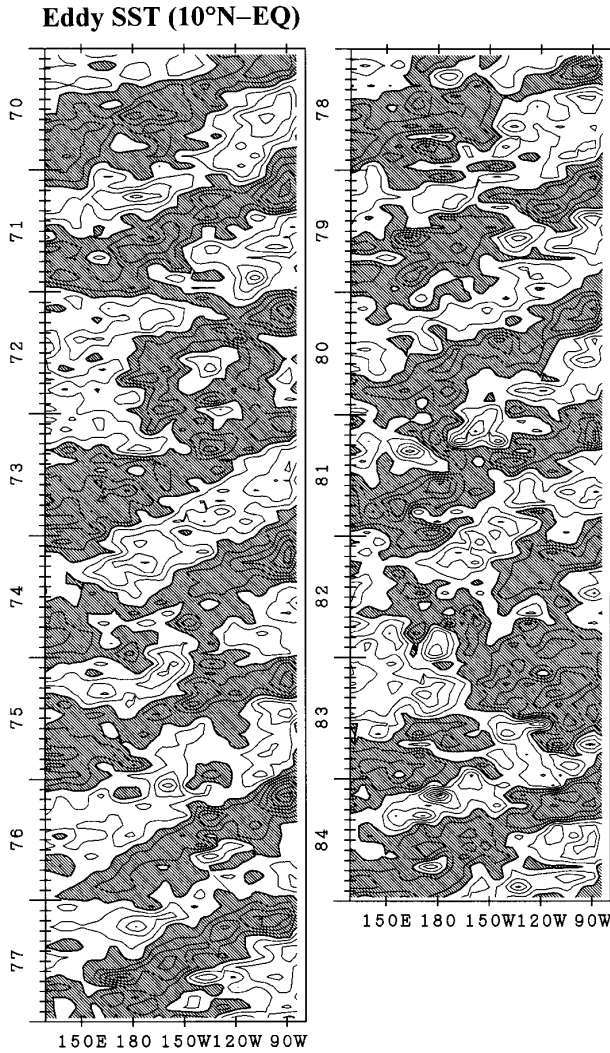


FIG. 5. Same as Fig. 2 but for the eddy SST at 10°N minus eddy SST at the equator. Contour interval is 0.5°C.

and western Pacific, respectively. Therefore, the eddy SST gradient, which is out of phase with the equatorial eddy SST, has positive anomalies in the western Pacific in the El Niño years. The simultaneous occurrences of the anomalous patterns in the eddy SST gradient and meridional wind associated with the El Niños indicate that a physically consistent relationship between wind and SST is observed, even in the presence of the El Niños.

As noted by Horel (1982), the eddy SST exhibits westward propagation near and south of the equator, but not north of the equator. This contrast between the Northern and Southern Hemispheres is reflected in a large eddy SST difference between the equator and 10°N (Figs. 6b,c), but not between the equator and 10°S (not shown), explaining why a significant propagating signal in the SST gradient is found north of the

equator. The propagating feature in the SST gradient results from the propagating SST perturbation along the equator, with minor contribution of the eddy SST at 10°N, whose amplitude is about one-third of the equatorial amplitude.

The correlation coefficient, in longitude and time, between the eddy meridional wind along 8°N and the eddy SST gradient between 10°N and the equator is 0.65 for the entire record period based on three-month running means, and the coefficient between the eddy meridional wind and equatorial eddy SST is  $-0.49$ . For these parameters, the decorrelation scales, at which the respective autocorrelation coefficients become zero, are 3.8–5.1 months in time, and 32°–44° in longitude. Therefore, there are  $120[\approx(15 \times 12/5.1) \times (150/44)]$  degrees of freedom for the data for 15 years for a 150° longitude strip, yielding a 95% significant correlation level of 0.18. Therefore, both the SST gradient and equatorial SST are significantly correlated with the meridional wind. Although the eddy SST at 10°N itself is not significantly correlated with the eddy meridional wind, the extraequatorial SST contributes to producing the higher correlation coefficient associated with the SST gradient than the coefficient associated with the equatorial SST alone. Furthermore, for the climatological monthly means, the correlation coefficient between the eddy SST gradient and eddy meridional wind is 0.76, and the coefficient between the equatorial eddy SST and eddy meridional wind is  $-0.52$ . Therefore, the SST gradient explains the one-half of the total variance of the climatological mean eddy meridional wind, but the equatorial SST, by itself, explains much less. Consequently, the SST along the equator is of primary importance in the propagating eddy meridional wind, with a secondary contribution from the SST in the Northern Hemisphere.

The high correlation coefficient between the eddy meridional wind and SST gradient does not, in itself, constitute proof of a causal linkage between the two parameters. The aforementioned physically consistent phase relationship between them, however, suggests that the eddy meridional wind is controlled by the SST gradient through boundary-layer processes. Furthermore, if the eddy meridional wind is not controlled by the eddy SST gradient, other forcings of the atmosphere must be responsible for the propagating feature in the meridional wind. This is unlikely the case. Convective heating might be as important as the SST gradient to force the surface wind fields. As a proxy for convective activity, outgoing longwave radiation (OLR) is widely used. However, it is known that the annual component of total OLR (without removing the zonally uniform component) propagates eastward along the equator (Murakami and Wang 1993) and along 10°N between 150°E and 120°W (Wang 1994a). We have also examined the eddy OLR field using OLR data between 1974 and 1987 (Gruber and Krueger 1984) but have not found any evidence of westward propagation of the

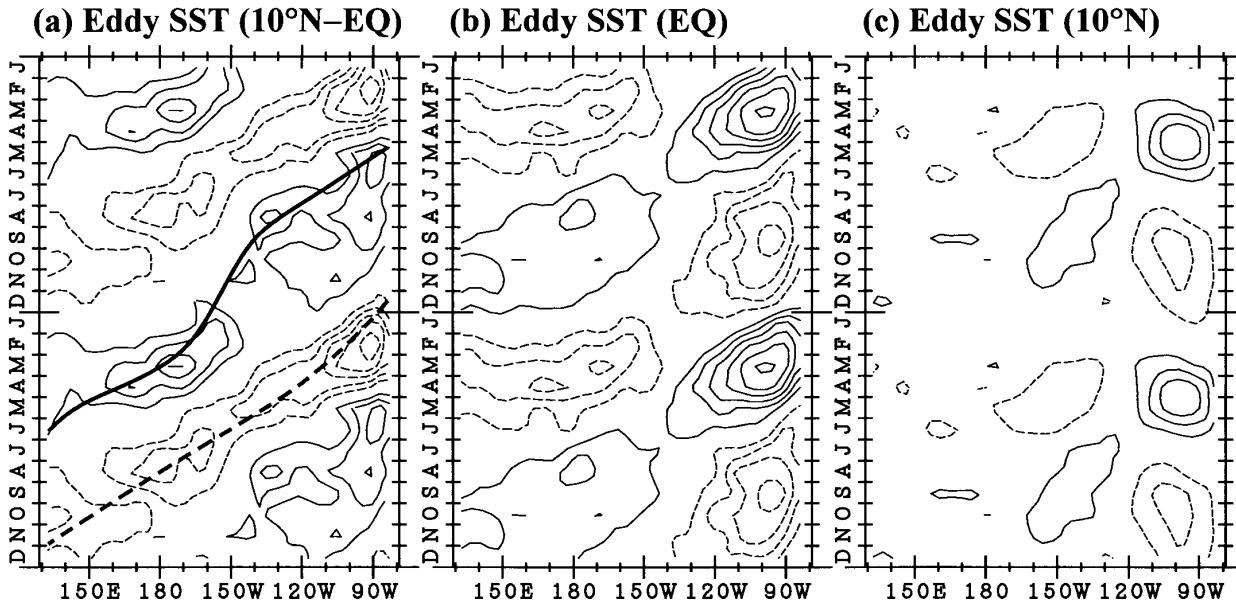


FIG. 6. Same as Fig. 3 but for (a) the eddy SST at  $10^{\circ}\text{N}$  minus eddy SST at the equator, (b) the eddy SST at the equator, and (c) the eddy SST at  $10^{\circ}\text{N}$ . Thick solid (dashed) curve in (a) indicates the positive (negative) maximum in the eddy meridional wind speed at  $8^{\circ}\text{N}$  shown in Fig. 3. Contour interval is  $0.3^{\circ}\text{C}$ , and zero contours are not shown.

annual signal. The energetic seasonal variation of the convection over the central America might be capable of forcing the meridional wind component independently of SST as demonstrated by Mitchell and Wallace (1992). However, the continental heating cannot solely cause the propagating signal over the basin at the annual period but is expected to force the standing oscillation in the eddy fields. Therefore, the variations in the meridional eddy wind is most likely to be due to the variations in the eddy SST field, regardless of whether or not the former significantly influences the latter.

In the central and eastern Pacific, it is well known that the equatorial SST propagation is associated with the seasonal development of the cold tongue (e.g., Horel 1982). In the western Pacific, however, the propagating feature is not clearly seen in the total SST; the annual phase propagation from the eastern Pacific along  $2^{\circ}\text{S}$ , the equator, and  $2^{\circ}\text{N}$  are detected as far as the date line,  $165^{\circ}\text{E}$ , and  $150^{\circ}\text{E}$ , respectively (not shown). On the other hand, the phases of the eddy SST propagate continuously toward the west as far as  $150^{\circ}\text{E}$  along all these latitudes. The difference in the propagating features between the total and eddy fields suggests that the propagating signals in the western Pacific are obscured by the zonally uniform components. Furthermore, the longitudinal continuity of the propagating feature to the east and west of the date line implies that the seasonal evolution of the cold tongue also produces the propagating feature in the western Pacific as well as in the central and eastern Pacific. The propagating character, however, is weaker in the western Pacific than in the central and eastern Pacific. The phase

change per unit longitude in the eddy SST gradient between  $150^{\circ}\text{E}$  and the date line is about one-half of that between the date line and South American coast. The weaker propagating feature probably reflects the smaller magnitude of the temperature variations associated with the cold tongue.

#### 4. Relationship to propagating signals in other parameters

It is interesting to examine the linkages between the propagating signal in the eddy meridional wind and the other propagating features previously reported. The propagation of the wind convergence along the equator reported by Horel (1982) can be shown to be related to the propagating feature in the eddy meridional wind speed along  $8^{\circ}\text{N}$ . The propagating signal in the equatorial eddy wind convergence is only a minor portion of the propagating signal of the eddy wind convergence centered along  $4^{\circ}\text{N}$  (Fig. 7a), as evidenced by the fact that the eddy wind convergence along the equator is in phase with that at  $4^{\circ}\text{N}$ , and the former has roughly 0.6 times smaller amplitude than the latter. Westward propagation along  $4^{\circ}\text{N}$  is evident to the east of the date line, and the eddy wind convergence along  $12^{\circ}\text{N}$  also propagates toward the west in the same region (Fig. 7b). The eddy wind convergence along  $4^{\circ}\text{N}$  ( $12^{\circ}\text{N}$ ) is out of phase (in phase) with the eddy meridional wind at  $8^{\circ}\text{N}$ . These phase relationships indicate that when the eddy meridional wind blows northward (southward), the eddy wind diverges within several degrees latitude to the south (north) and converges to the north (south)

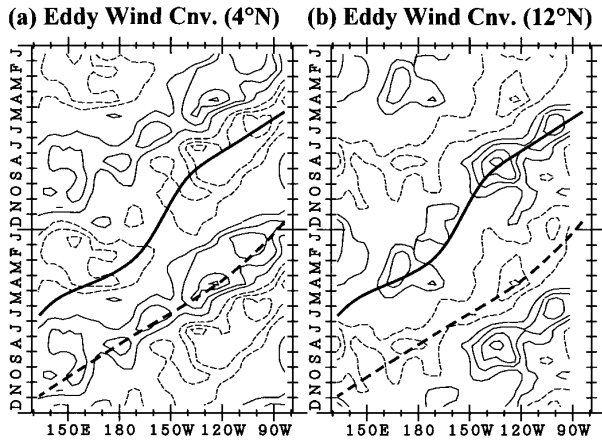


FIG. 7. Same as Fig. 3 but for the eddy wind convergence along (a) 4°N and (b) 12°N. Contour interval is  $1.0 \times 10^{-6} \text{ s}^{-1}$ , and zero contours are not shown.

of 8°N, respectively. The wind convergence in the Tropics is mainly contributed by the meridional wind speed because the meridional length scale is much narrower than the zonal length scale. The meridional scale around 8°N is especially narrow to the east of the date line as shown in Fig. 1, associated with the presence of the intertropical convergence zone (ITCZ). Therefore, the propagating signal of the eddy meridional wind along 8°N reflects in the propagating signal in the eddy wind convergence at 4° and 12°N to the east of the date line, though the eddy anomaly in the meridional wind continuously propagates across the entire basin.

Mitchum and Lukas (1990) found a bimodal feature in the annual westward propagating signal in sea level displacements in the western Pacific around 7°N based on island tide gauge data. They showed that the annual phase of the sea level displacement propagates westward in non-El Niño periods, whereas in the El Niño periods the phase is longitudinally uniform. The propagation speed was estimated as  $0.5 \text{ m s}^{-1}$  and was the same as the propagation speeds of the equatorial zonal wind and eddy meridional wind at 8°N. Mitchum and Lukas (1990) hypothesized that the westward propagating feature in the sea level displacement results from the resonantly forcing by the westward propagating wind field. Furthermore, based on the fact that the similar interannual modulation is observed in the equatorial zonal wind, they suggested that the interannual modulation in the propagating wind field causes the bimodal feature of the propagating signal in the sea level displacement. As shown in the previous section, the propagations in the eddy meridional wind speed at 8°N are also seen only in the non-El Niño years in the western Pacific. The qualitative agreement in the interannual modulation of the propagating signals between the equatorial zonal wind and eddy meridional wind at 8°N suggests the existence of a relationship between

these two fields. Therefore, we speculate that the westward propagations in the two wind fields are the two aspects of a single westward propagating phenomenon.

## 5. Summary and discussion

We have shown that a prominent and well-organized annual westward propagating signal is detectable in the longitudinally dependent component of the meridional wind speed along 8°N across the Pacific Ocean. The propagating signal in the eddy meridional wind has larger amplitude than the well-known westward propagating zonal wind component along the equator. The mechanism responsible for the seasonal variation of the eddy meridional wind speed is most likely to be the boundary-layer baroclinity induced by the SST variations. This interpretation is supported by the high correlation coefficients between the eddy meridional SST gradient to the north of the equator and eddy meridional wind and by the consistent relationship between these two parameters observed in individual years.

The existence of the atmospheric propagating feature in the Northern Hemisphere is attributed to the propagating eddy SST along the equator and in the Southern Hemisphere. However, it is not explained why the SST propagation is seen in the Southern Hemisphere and not in the Northern Hemisphere. In order to answer this question, further investigations on the seasonal SST changes are necessary by two approaches. One approach is to clarify the mechanisms of the seasonal SST response forced by local or remote atmospheric forcings. The other is to investigate the SST and wind variations from the point of view of the air-sea coupled system since the effect of the seasonal SST changes on the atmospheric variations cannot be ignored.

Although the propagating feature of the equatorial SST have previously been considered to affect atmospheric variations in a narrow band within a few degrees from the equator, the present results indicate that the equatorial SST induces propagating features in the atmospheric variations as far north as 12°N. This result emphasizes the importance of the SST propagation for the understanding of the air-sea coupled processes on the seasonal timescale. Therefore, the mechanism responsible for the annual westward propagation of the SST anomaly is of particular interest. Recently, Chang (1994) suggested that the wind forcing plays an essential role for the SST propagation along the equator, although the surface heat flux forcing dominates the seasonal cycle of SST in most areas of the tropical Pacific. Xie (1994a) proposed a linear theory in which the interaction between the ocean mixed layer and atmospheric boundary layer is responsible for the equatorial westward propagation in both the zonal wind stress and SST. Using a linear model, Minobe and Takeuchi (1995) showed that the oceanic first meridional mode Rossby wave is important for the SST propagation in the central Pacific through the zonal SST advection.

The SST change in the Southern Hemisphere, where the annual eddy SST component also exhibits the westward propagation, cannot be attributed to the oceanic responses associated with either the equatorial waves or equatorial upwelling. Mitchell and Wallace (1992) attributed the broad SST cooling  $\sim 10^{\circ}\text{S}$  in the tropical Pacific from August to October to the increases and spreading of stratocumulus cloud decks. They noted the possibility of the feedback processes between the SST and cloud cover.

Recently, using linear eigenmode analyses, Chang and Philander (1994) showed that an unstable mode contributes to the westward propagating feature in the annual cycle of near-equatorial zonal wind and SST. This mode has the symmetric meridional profiles of the SST and zonal wind anomalies and antisymmetric meridional wind anomaly. In the present study, however, the meridional structure of the propagating signal in the eddy fields exhibits significant asymmetry about the equator. The asymmetry of the propagating features probably reflects the asymmetry in the mean states of the tropical atmosphere and ocean; that is, the ITCZ exists in the Northern Hemisphere over the relatively warm SST region in the central and eastern Pacific. The asymmetries in the mean states arise from the air–sea interaction (Xie and Philander 1994; Xie 1994b), and modify the seasonal evolution of the SST and wind fields from that without the asymmetric mean states (e.g., Mitchell and Wallace 1992). Therefore, it is important to examine how the asymmetry of the mean states with respect to the equator affect the annual westward propagating signal in theoretical or model studies. Recently, air–sea coupled general circulation models (CGCMs) simulated the realistic seasonal variation forced by only external solar forcing (e.g., Nagai et al. 1992). It would be of interest to analyze the eddy fields produced by the CGCMs to study the mechanism of the propagating signals.

Although essential features of the propagating signal in the eddy fields might be explained by a single air–sea coupled mode, the mode might interact other air–sea coupled modes. Wang (1994b) analyzed the observed wind and SST fields in the central and eastern tropical Pacific in terms of the symmetric and antisymmetric components. He pointed out that the propagating symmetric mode (symmetric SST and zonal wind with antisymmetric meridional wind), which is responsible for the equatorial SST propagation, is regulated by the nonpropagating antisymmetric mode. The antisymmetric mode is forced by annual cycle in the differential solar insolation between the Northern and Southern Hemispheres. In order to explain the complex nature of the seasonal evolution of the tropical atmosphere and oceans, such interactions between the different coupled modes should be taken into account in further investigations.

*Acknowledgments.* I would like to express my sincere thanks to Sei-ichi Kanari, Kensuke Takeuchi, Toshiyuki Hibiya, Tetsuo Nakazawa, and Edward Sarachik for invaluable discussions and to Todd Mitchell for reading this manuscript in the original form. The comments by anonymous reviewers that contributed to a significant improvement of the paper are appreciated.

#### REFERENCES

- Bjerknes, J., 1961: El Niño study based on analysis of ocean surface temperature. *Inter-Amer. Trop. Tuna Comm. Bull.*, **5**, 219–212.
- Chang, P., 1994: A study of the seasonal cycle of sea surface temperature in the tropical Pacific Ocean using reduced gravity models. *J. Geophys. Res.*, **99**(C4), 7725–7741.
- , and S. G. H. Philander, 1994: A coupled ocean–atmosphere instability of relevance to the seasonal cycle. *J. Atmos. Sci.*, **51**, 3627–3648.
- Goldenberg, S. B., and J. J. O'Brien, 1981: Time and space variability of tropical Pacific wind stress. *Mon. Wea. Rev.*, **109**, 1190–1297.
- Gruber, A., and A. F. Krueger, 1984: The status of the NOAA outgoing longwave radiation dataset. *Bull. Amer. Meteor. Sci.*, **65**, 958–962.
- Horel, J., 1982: On the annual cycle of the tropical Pacific atmosphere and ocean. *Mon. Wea. Rev.*, **110**, 1863–1878.
- Lindzen, R. S., and S. Nigam, 1987: On the role of sea surface temperature gradients in forcing low-level winds and convergence in the tropics. *J. Atmos. Sci.*, **44**, 2418–2436.
- Lukas, R., and E. Firing, 1985: The annual Rossby wave in the central equatorial Pacific Ocean. *J. Phys. Oceanogr.*, **15**, 55–67.
- Meehl, G. A., 1990: Seasonal cycle forcing of El Niño–Southern Oscillation in a global coupled ocean–atmosphere GCM. *J. Climate*, **3**, 72–98.
- Meyers, G., 1979: Annual variation in the slope of the  $14^{\circ}\text{C}$  isotherm along the equator in the Pacific Ocean. *J. Phys. Oceanogr.*, **9**, 885–891.
- Minobe, S., and K. Takeuchi, 1995: Annual period equatorial waves in the Pacific Ocean. *J. Geophys. Res.*, **100**(C9), 18 379–18 392.
- Mitchell, T. P., and J. M. Wallace, 1992: The annual cycle in equatorial convection and sea surface temperature. *J. Climate*, **5**, 1140–1156.
- Mitchum, G. T., and R. Lukas, 1990: Westward propagation of annual sea level and wind signals in the western Pacific Ocean. *J. Climate*, **3**, 1102–1110.
- Murikami, T., and B. Wang, 1993: Annual cycle of equatorial east–west circulation over the Indian and Pacific oceans. *J. Climate*, **6**, 932–954.
- Nagai, T., T. Tokioka, M. Endoh, and Y. Kitamura, 1992: El Niño–Southern Oscillation simulated in an MRI atmosphere–ocean coupled general circulation model. *J. Climate*, **5**, 1202–1233.
- Philander, S. G. H., 1990: *El Niño, La Niña and the Southern Oscillation*. Academic Press, 293 pp.
- , and Y. Chao, 1991: On the contrast between the seasonal cycles of the equatorial Atlantic and Pacific Oceans. *J. Phys. Oceanogr.*, **21**, 1399–1406.
- Reynolds, R. W., 1983: A comparison of sea surface temperature climatologies. *J. Climate Appl. Meteor.*, **22**, 447–458.
- Sadler, J. C., M. A. Lander, A. M. Hori, and L. K. Oda, 1987: *Tropical Marine Climatic Atlas*. Vol. 2, *Pacific Ocean*. University of Hawaii, 27 pp.
- Wang, B., 1994a: Climatic regimes of tropical convection and rain fall. *J. Climate*, **7**, 1109–1118.
- , 1994b: On the annual cycle in the tropical eastern-central Pacific. *J. Climate*, **7**, 1926–1942.
- Wyrtki, K., and G. Meyers, 1976: The trade wind field over the Pacific Ocean. *J. Appl. Meteor.*, **15**, 698–704.
- Xie, S.-P., 1994a: On the genesis of equatorial annual cycle. *J. Climate*, **7**, 2008–2013.
- , 1994b: The maintenance of an equatorially asymmetric state in a hybrid coupled GCM. *J. Atmos. Sci.*, **51**, 2602–2612.
- , and S. G. H. Philander, 1994: A coupled ocean–atmosphere model of relevance to the ITCZ in the eastern Pacific. *Tellus*, **46A**, 340–350.